



Kinetic analysis and CFD simulations of the photocatalytic production of hydrogen in silicone microreactors from water-ethanol mixtures



Alejandra Castedo ^a, Irantzu Uriz ^b, Lluís Soler ^a, Luis M. Gandía ^{b,c}, Prof. Jordi Llorca ^{a,*}

^a Institute of Energy Technologies and Centre for Research in Nanoengineering, Universitat Politècnica de Catalunya, Diagonal 647, 08028 Barcelona, Spain

^b Departamento de Química Aplicada, Edificio de los Acebos, Universidad Pública de Navarra, Campus de Arrosadía s/n, E-31006 Pamplona, Spain

^c Institute for Advanced Materials (InaMat), Universidad Pública de Navarra, E-31006 Pamplona, Spain

ARTICLE INFO

Article history:

Received 20 July 2016

Received in revised form 3 October 2016

Accepted 8 October 2016

Available online 11 October 2016

Keywords:

Hydrogen photoproduction

Gas-phase photocatalysis

Microreactor

Kinetic modeling

Computational fluid dynamics (CFD)

ABSTRACT

Silicone microreactors containing microchannels of 500 μm width in a single or triple stack configuration have been manufactured, coated with an Au/TiO₂ photocatalyst and tested for the photocatalytic production of hydrogen from water-ethanol gaseous mixtures under UV irradiation. Computational fluid dynamics (CFD) simulations have revealed that the design of the distributing headers allowed for a homogeneous distribution of the gaseous stream within the channels of the microreactors. A rate equation for the photocatalytic reaction has been developed from the experimental results obtained with the single stack operated under different ethanol partial pressures, light irradiation intensities and contact times. The hydrogen photoproduction rate has been expressed in terms of a Langmuir-Hinshelwood-type equation that accurately describes the process considering that hydrogen is produced through the dehydrogenation of ethanol to acetaldehyde. This equation incorporates an apparent rate constant (k_{app}) that has been found to be proportional to the intrinsic kinetic rate constant (k), and that depends on the light intensity (I) as follows: $k_{\text{app}} = k \cdot I^{0.65}$. A three-dimensional isothermal CFD model has been developed in which the previously obtained kinetic equation has been implemented. The model adequately describes the production of hydrogen of both the single and triple stacks. Moreover, the specific hydrogen productions (i.e. per gram of catalyst) are very close for both stacks thus suggesting that the scaling-up of the process could be accomplished by simply numbering-up. However, small deviations between the experimental and predicted hydrogen production suggest that a fraction of the radiation is absorbed by the microreactor components which should be taken into account for scaling-up purposes.

© 2016 Elsevier B.V. All rights reserved.

1. Introduction

Photocatalytic water-splitting using TiO₂ offers a promising way for realizing clean, low-cost and environmentally friendly production of hydrogen by using mainly water, biomass, and solar energy [1,2]. Since Fujishima and Honda first demonstrated the photocatalytic water splitting using TiO₂ as the catalyst in 1972 [3], semiconductor photocatalysis has drawn much attention. Extensive efforts have been made to develop the most significant applications of photocatalysis, particularly solar water splitting and the purification of water and air. Two important issues are the main focus of current research in photocatalysis, namely the development of efficient visible light-driven photocatalysts and the

design of photocatalytic reactors with optimized photon and mass transfer [4]. Concerning the design of reactors, optofluidic devices made out of quartz or Pyrex with microchannels made by either micro-milling, etching processes or laser ablation with immobilized catalyst have been proposed to overcome photon transfer limitations suffered by slurry systems, for instance [5]. Optofluidic devices are commonly employed in water treatment processes [6] and they have recently started to be considered for hydrogen production through liquid-phase reactions [7]. In contrast, studies focused on gas-phase heterogeneous photocatalysis are scarce and they are mainly related to air purification [8,9].

Microreactors appear as suitable tools to perform photocatalytic reactions due to their promising characteristics, such as the improvement of mass and photon transfer towards the photocatalyst, flow control, large surface-area-to-volume ratios, high spatial illumination homogeneity and good light penetration, among other valuable features. Nevertheless, there are several aspects that still require to be improved in photocatalytic microreactors, such as

* Corresponding author at: Institut de Tècniques Energètiques, Universitat Politècnica de Catalunya, Av. Diagonal 647, Ed. ETSEIB 08028, Barcelona, Spain.

E-mail address: jordi.llorca@upc.edu (J. Llorca).

better photonic efficiency or the use of cheaper fabrication materials and procedures with the aim of decreasing the overall cost of the photoproduced hydrogen. In order to maximize the reactant-catalyst contact and the illumination efficiency, two microreactor systems have been developed by our group, where gas-solid reactions were conducted for the photogeneration of hydrogen using water-ethanol gaseous mixtures and an Au/TiO₂ photocatalyst. One of them consisted on a honeycomb photoreactor with optical fibers inside the honeycomb cells [10–12], where an excellent photon delivery was achieved. More recently, we have manufactured a silicone microreactor with microchannels using a simple, versatile and cheap technology based on 3D printing and polydimethylsiloxane (PDMS) polymerization. The main advantage of the latter is that it allows the use of sunlight directly, which obviously reduces the hydrogen production costs [13].

According to the literature, the design of photoreactors is often based on efficiency parameters (e.g. quantum yield and photonic efficiency) [4]. In contrast, very few studies exploit kinetic aspects for accurate modeling which is also important for process development and scale-up. Indeed, the development of kinetic models and an accurate determination of their parameters are also important for photoreactor modeling and optimization. It is worth mentioning that a big challenge concerning the kinetic modeling of the photocatalytic reactions is to assess the influence of the light intensity on the reaction rate [14].

Computational fluid dynamics (CFD) is being increasingly employed for the analysis and design of chemical processes equipment. CFD is a computer simulation tool that allows predicting the behavior of a chemical reactor, for example, provided that the model has been validated before by a good accordance between the experimental and simulated results [15]. In this work we report for the first time on a CFD model capable of simulating the photocatalytic gas-phase production of hydrogen from water-ethanol mixtures in a microchannel reactor under different operational conditions. The model incorporates a kinetic rate equation of the reaction developed on the basis of experimental results obtained using a single-stack silicone microreactor loaded with an Au/TiO₂ catalyst. The model has been validated using the results obtained with a triple-stack silicone microreactor. The results demonstrated the good performance and scale-up possibilities of silicone microreactors for photocatalytic renewable hydrogen production.

2. Experimental section

2.1. Experimental setup

Fig. 1 shows the devices manufactured in this work to carry out the photocatalytic production of hydrogen and the physical models of the fluidic domains developed to conduct the CFD simulations. The single silicone microreactor and the scheme of its fabrication has been reported previously [13]. Briefly, the PDMS microreactor shown in Fig. 1A consisted on nine microchannels of 500 μm (width) \times 1 mm (depth) \times 47 mm (length), with a total volume of 0.21 cm^3 , and two headers to facilitate gas distribution. A suspension of Au/TiO₂ in ethanol was prepared and deposited onto the bottom wall of the microchannels to reach a catalyst loading of ca. 2.4 mg cm^{-2} . Au/TiO₂ was prepared by incipient wetness impregnation over commercial TiO₂ (Degussa P90) from a toluene solution containing pre-formed Au nanoparticles (4 nm in diameter, final metal loading of 1.8 wt.%). An optimum Au loading for the photoreaction of 1–2 wt.% was reported in previous studies [11,16,17]. The photocatalyst was calcined at 673 K for 2 h (2 K min^{-1}) to eliminate the protecting shell around the Au nanoparticles used to prevent agglomeration and also to ensure a good contact between Au and

TiO₂. [18]. After depositing the photocatalyst into the microchannels, the photomicroreactor was sealed with a PDMS cover using a corona plasma treatment (BD-20AC Electro-Technic Products).

The triple stack microreactor is shown in Fig. 1B. It was fabricated with the channels slightly shifted to ensure light exposure to all of the microchannels. The total number of channels was 25 and their dimensions were the same as those of the single stack microreactor. Although this system is an interesting route to attain process intensification (PDMS is optically transparent down to 240 nm), it must be taken into account that as the PDMS components become thicker, more light is absorbed. The radiation power was measured using a UV-A sensor (model PMA 2110, Solar Light Co.), which registers UV radiation within spectral response 320–400 nm, connected to a radiometer (model PMA2200, Solar Light Co.), which gives the measured irradiance in mW cm^{-2} .

The microreactors were irradiated with two high-efficacy LEDs emitting at $365 \pm 2 \text{ nm}$ (LED Engin LZ1-10U600) connected to an adjustable regulated DC power supply (Grelco, model G1307). The radiation intensity at the photocatalytic surface was varied between 0 and 23 mW cm^{-2} by tuning the current-voltage output of the power supply. We selected this range of UV-A irradiance in order to work in a similar order of magnitude than that of sunlight radiation in our area, which shows an average value of 4 mW cm^{-2} (measured at midday). Photocatalytic experiments were carried out at atmospheric pressure and room temperature under dynamic conditions. The experimental set up consisted of an argon stream bubbled through a saturator containing different mixtures of water and ethanol (>99.9%, Scharlau). The gaseous mixture was directly introduced into the microreactor, which was previously flushed with an Ar stream. The effluent was monitored online every 3.5 min with an Agilent 490 Micro gas chromatograph equipped with MS 5 Å, Plot U and Stabilwax columns for a complete analysis of the products.

Photocatalytic tests in the single PDMS microreactor were conducted using water:ethanol ($\text{H}_2\text{O:EtOH}$) mixtures of 99:1, 90:10, 80:20, 65:35, 50:50 and 25:75 (molar basis) at a residence time of 0.35 s (gas-hourly space velocity GHSV of 10,200 h^{-1}). In addition, different space velocities were also tested (13,700, 7600 and 4600 h^{-1}) using a $\text{H}_2\text{O:EtOH}$ mixture of 90:10 to assess possible mass transfer limitations. The triple stack PDMS microreactor was tested using $\text{H}_2\text{O:EtOH}$ mixtures of 99:1, 90:10, 80:20 and 50:50 at a residence time of 0.98 s (GHSV = 3700 h^{-1}).

2.2. Photocatalyst characterization

The microchannels and the deposition of the Au/TiO₂ catalyst on their walls were studied by scanning electron microscopy (SEM) with a Zeiss Neon40Crossbeam Station equipped with a field emission electron source. As reported previously, the photocatalyst was also characterized by X-ray diffraction (XRD), UV-vis reflectance spectroscopy, transmission electron microscopy (TEM) and X-ray photoelectron spectroscopy (XPS) [13].

2.3. Data analysis

The kinetic experiments were conducted under differential conditions, at ethanol conversions well below 5%. The only reaction products detected were hydrogen and acetaldehyde in a nearly stoichiometric proportion, thus indicating that the overall reaction was the dehydrogenation of ethanol into acetaldehyde and hydrogen: $\text{CH}_3\text{CH}_2\text{OH} \rightarrow \text{CH}_3\text{CHO} + \text{H}_2$.

Under the mentioned conditions, the rate of hydrogen photo-production R_{H_2} can be obtained according to

$$R_{\text{H}_2} = \frac{F_{\text{H}_2}}{W_C} \quad (1)$$

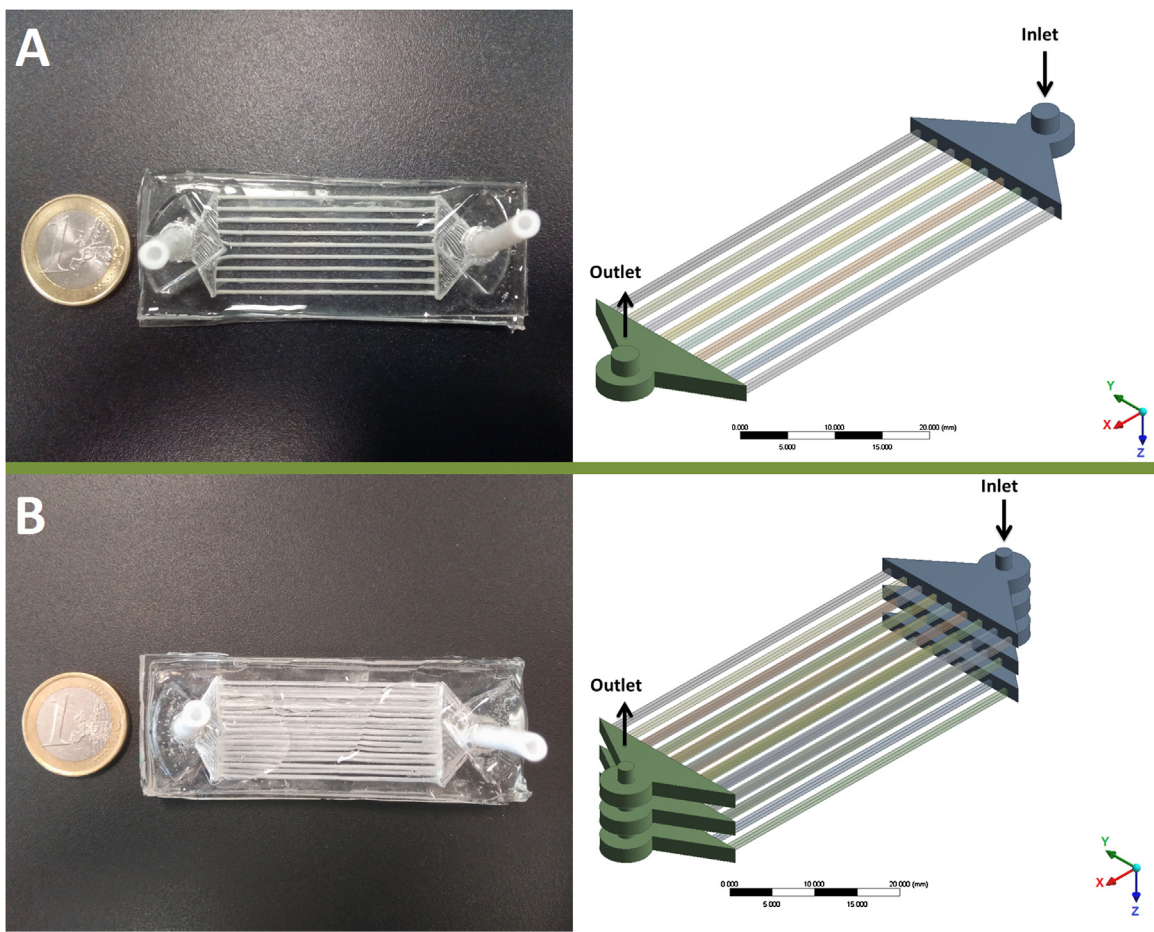


Fig. 1. Photograph and CFD physical model (fluidic domain) of the single stack PDMS microreactor (A). Photograph and CFD physical model (fluidic domain) of the triple stack PDMS microreactor (B).

where F_{H_2} is the molar flow of hydrogen photogenerated and W_c is the mass of catalyst loaded into the microreactor.

The reaction rate data were fitted to the kinetic model by means of nonlinear regression analysis using a modified Levenberg–Marquardt algorithm provided by subroutine DRNLIN in the IMSL library. This algorithm allowed minimizing the objective function for the normalized residual sum of squares (NRSS),

$$NRSS = \sum_{n=1}^N \left(\frac{R_{e,n} - R_n}{R_n} \right)^2 \quad (2)$$

where $R_{e,n}$ is the reaction rate estimated by the model, R_n corresponds to the n value of the experimentally measured hydrogen production rate according to Eq. (1) and N is the total number of experiments.

2.4. CFD modeling

The mass, species and momentum transport equations were solved in isothermal conditions at steady state using the commercial CFD software package ANSYS® CFX on a Lenovo dual-processor Intel® Xenon® ThinkStation D20 workstation running MS Windows 7 Professional® x64 with an available RAM of 64.0 GB. In the case of the microchannels, two-dimensional meshes were developed and extruded along the longitudinal axis. The geometry was meshed using prismatic and hexahedral elements giving a computational unstructured grid. A higher density of elements was created near the walls, where the photochemical reaction takes place. The flow distributing headers were meshed and modeled as described in a previous work [19]. In order to check that the solutions were

independent of the grid used, two meshes were considered for the single stack reactor. The first one included a total of 425,000 vol elements and the second had 712,000 elements. Both grids provided the same results even though very small differences appeared only at very high space velocities (above 40,000 h^{-1}); therefore, the grid with fewer volume elements was used throughout this work to reduce the computation time. The triple stack reactor was meshed following the same scheme as for the single stack microreactor.

3D simulations were conducted assuming that a thin layer of the Au/TiO₂ catalyst was uniformly deposited onto the microchannels (2.4 mg cm^{-2}). The photochemical reaction rate expression was implemented in the CFD model. The catalytic reaction was modeled considering the bottom walls of the microchannels as sources of products and sinks of reactants. The non-slip boundary condition was selected at the surface of the microchannels. Mass transfer within the catalytic layer was neglected due to its very small depth.

Criteria of convergence were based on the residuals, which were defined as the normalized square root (RMS) of the difference between the latest solution and the running arithmetic average of the variables. The RMS value selected was 10^{-6} to obtain a good convergence. The imbalance level of the conservation equations after convergence was typically below 0.1%.

3. Kinetic analysis

The rate equations used to describe photocatalytic reactions are usually based on simple power-law expressions of the type

$$R = k' Cl^\alpha \quad (3)$$

where R is the reaction rate, k' is the rate constant that is independent on the light intensity I , C is the concentration of a reactant and α is an exponent that depends on the efficiency of the electron-hole formation and recombination processes. Many studies have reported values of α between 0.5 and 1 depending on the light intensity. According to Herrmann and Puzenat [20], the rate determining step is normally the reaction between the adsorbed species. However, TiO_2 is a n-type semiconductor and the photo-induced holes are much less numerous than electrons at low intensities, making hole formation the limiting step and the reaction rate directly proportional to the light intensity. In contrast, at high intensities the concentrations of both electrons and holes are high, so the rate of electron-hole formation becomes greater than the photocatalytic reaction rate, which favors electron-hole recombination, and the rate then becomes proportional to the square root of the light intensity. Due to the importance of this kinetic parameter, α must be determined experimentally in each case because its value is affected by the characteristics of the photocatalytic device used.

Kinetic expressions of the Langmuir-Hinshelwood (L-H) type are considered in the field of heterogeneous photocatalysis. Pruden and Ollis were among the first working on the kinetics of TiO_2 photocatalyzed reactions [21]. In this work, the following L-H type rate equation has been adopted to describe the rate of hydrogen production:

$$R_{H_2} = \frac{k_{app} K P_{EtOH}}{1 + K P_{EtOH}} \quad (4)$$

where P_{EtOH} is partial pressure of EtOH, K may be considered as an equilibrium pseudo constant, and k_{app} is an apparent kinetic constant that depends on the intrinsic kinetic constant k and the light intensity I as follows [22]:

$$k_{app} = k I^\alpha \quad (5)$$

4. Results and discussion

4.1. Single stack PDMS microreactor

4.1.1. Fluid flow distribution

Due to the great influence of the residence time distribution on the reactor performance a series of CFD simulations were first conducted to investigate the distribution of the gaseous stream in the microchannels of the single stack microreactor. Several cases at different flow rates were simulated numerically under reaction conditions ($I = 1.5 \text{ mW cm}^{-2}$) using a water-ethanol gaseous mixture of 90:10 (molar basis) at GHSV values ranging from 2900 to 41,000 h^{-1} .

As a representative example of the results obtained, Fig. 2A shows the field of velocities resulting at $\text{GHSV} = 10,200 \text{ h}^{-1}$ in the whole fluidic domain of the single stack microreactor. It can be seen that the flow distribution is very homogeneous with average velocity values of $0.254 \pm 0.002 \text{ m s}^{-1}$ at the entrance of each channel. Fig. 2B shows the velocity profiles along a central line perpendicular to the main flow at the microchannels entry. Obviously, the velocity is 0 in contact with the solid walls that separate the channels. The profiles are shown for two space velocities (10,200 and 41,000 h^{-1}). It can be seen that the velocity profiles are very similar for the 9 microchannels and that they are parabolic, in accordance with the laminar regime governing the flow at the considered conditions.

According to the CFD simulations, it can be concluded that the simple design of the headers used (with an inlet perpendicular to the microchannels and a relatively small distribution and diffusion chamber) provides a well-developed and uniform flow distribution in the microchannels. The outlet section design is less demanding due to the very small gas velocities prevailing in this section. Using

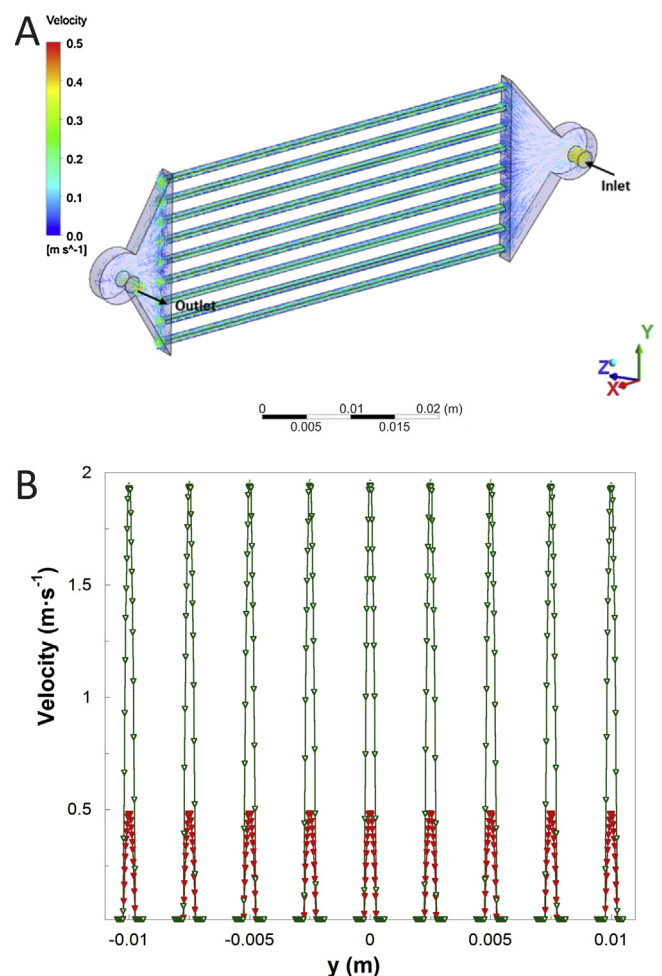


Fig. 2. Velocity field in the fluidic domain of the single stack microreactor at GHSV of $10,200 \text{ h}^{-1}$ (A). Velocity profiles along a central line perpendicular to the main flow at each microchannel entry in the single stack microreactor at GHSV of $41,000 \text{ h}^{-1}$ (open symbols) and $10,200 \text{ h}^{-1}$ (filled symbols) (B).

the same geometry as for the entry section, a very uniform flow is achieved at the microreactor exit and no recirculation is created.

4.1.2. Mass transfer limitations

The photocatalytic layer was examined by SEM in order to study its distribution, homogeneity and average thickness. Fig. 3A shows a representative micrograph of the cross-section of a microchannel. A well-developed and homogeneous Au/TiO_2 layer coating the microchannel wall is perfectly visible, with an average thickness of roughly $8 \pm 2 \mu\text{m}$. At higher magnification (Fig. 3B) it is possible to observe that the photocatalyst layer is composed of individual particles with a narrow particle size distribution centered at about 20 nm. Due to the very small thickness of the catalytic layer, internal mass transport limitations have been not included in the mathematical model, as explained before [23,24].

As for the external mass transport limitations, they are already accounted for the CFD model by the convective and diffusive terms of the conservation equations. Consequently, several photoreaction tests were carried out at different space velocities under different light intensities. The hydrogen photogeneration rates (R_{H_2}) obtained are shown in Fig. 4. The results demonstrate a minor influence of the external mass transport limitations. The measured specific rate of hydrogen production increases with the light intensity, as expected, but for a given light intensity it remains almost unchanged as the space velocity varies. Only at GHSV values above

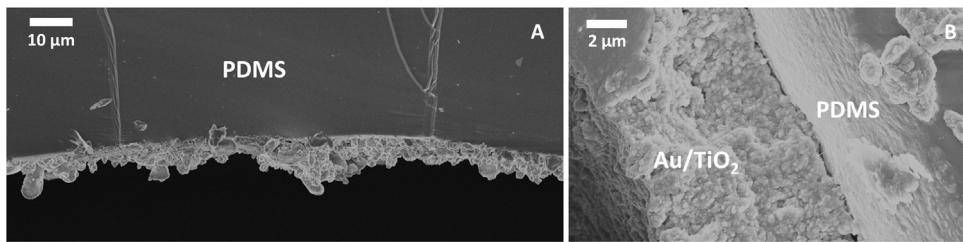


Fig. 3. Representative SEM image of the Au/TiO₂ photocatalyst layer deposited on the microchannels (A). High magnification SEM image of the Au/TiO₂ photocatalyst layer on the microchannels (B).

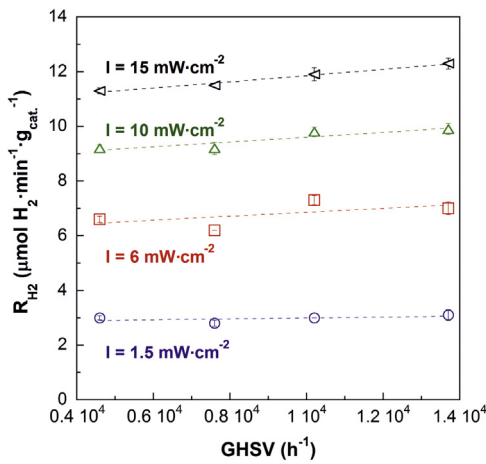


Fig. 4. Effect of the GHSV on the H₂ photoproduction rates using a water-ethanol gaseous mixture of 90:10 (molar basis) at different light intensity values. The error bars were calculated from the results of 4 replicates.

10,000 h⁻¹ there is a slight increase in the hydrogen production rate as the space velocity increases, thus pointing towards a minor impact of the mass transport on the hydrogen production. This effect seems to be slightly more important at increasing irradiances, likely due to faster photochemical kinetics.

4.1.3. Kinetic model

The experimental values of the rates of hydrogen production obtained at different partial pressures of ethanol in the reactor feed stream (corresponding to water-ethanol gaseous mixtures with ethanol molar contents ranging from 1% to 75%) and different light intensities are shown in Fig. 5. The experiments were performed at a residence time of 0.35 s (GHSV = 10,200 h⁻¹). As can be seen in Fig. 5, for a given ethanol partial pressure in the feed stream, the reaction rate continuously increased with the light intensity. On the other hand, for a given light intensity, the H₂ photoproduction rate increased sharply until an ethanol partial pressure of approximately 0.30 kPa was achieved (corresponding to about 10 mol% of ethanol in the feed stream). A further increase of the ethanol partial pressure gives rise to a small increase of the hydrogen production rate that seems to achieve an almost constant value at very high ethanol contents. This behavior is very well described by a Langmuir-Hinshelwood equation such as the one given by Eqs. (4) and (5) as judged from the good fit of this model to the experimental results (see solid lines in Fig. 5). The best fit was obtained with the following values of the kinetic parameters at 95% confidence level: $\alpha = 0.65 \pm 0.03$; $K = 16 \pm 2 \text{ kPa}^{-1}$; $k = 2.8 \pm 0.2 (\mu\text{mol H}_2 \text{ cm}^{1.3}) \cdot (\text{min}^{-1} \text{ g}_{\text{cat}}^{-1} \text{ mW}^{-0.65})$. The normalized residual sum of squares (NRSS) was 0.18. The value of the exponent α is within the expected range of 0.5–1.

This kinetic model was implemented in the developed CFD code to simulate the performance of the single stack microreactor at

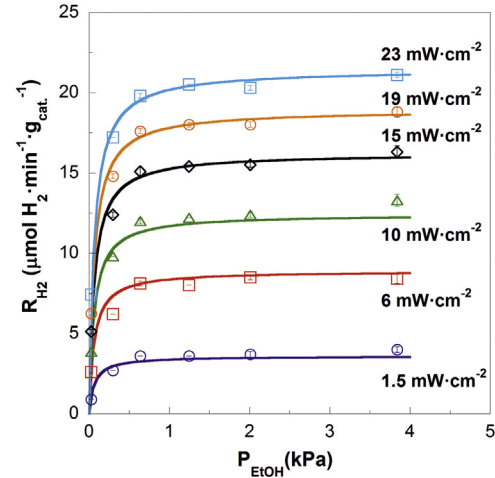


Fig. 5. Effect of the partial pressure of ethanol on H₂ photoproduction rates in a single stack microreactor at GHSV of 10,200 h⁻¹ and different light intensity values. The error bars were calculated from the results of 4 replicates. The symbols correspond to the experimental results and the lines to the kinetic model given by Eqs. (4) and (5) (see text).

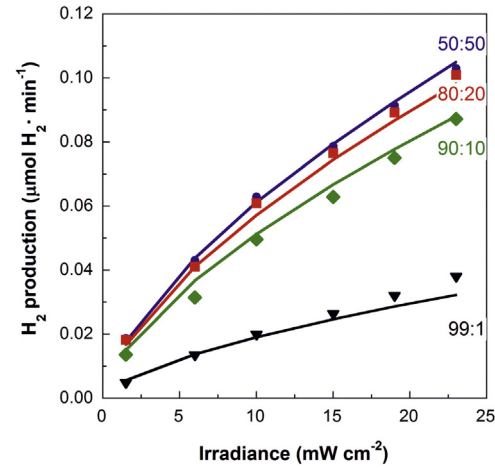


Fig. 6. Hydrogen photoproduction rates in the single stack microreactor at different light irradiance values and H₂O:EtOH molar ratios for GHSV = 10,200 h⁻¹. The symbols correspond to the experimental results and the lines to the CFD simulations.

varying feed stream compositions and light irradiances. The experimental values of the hydrogen photoproduced by the stack and those given by the CFD simulations are compared in Fig. 6. It can be seen that a good accordance exists between the experimental and the simulated results, thus indicating that the CFD model developed describes accurately the single stack microreactor. The results clearly show that the hydrogen photoproduction increased when the irradiance was increased, which suggests that the reac-

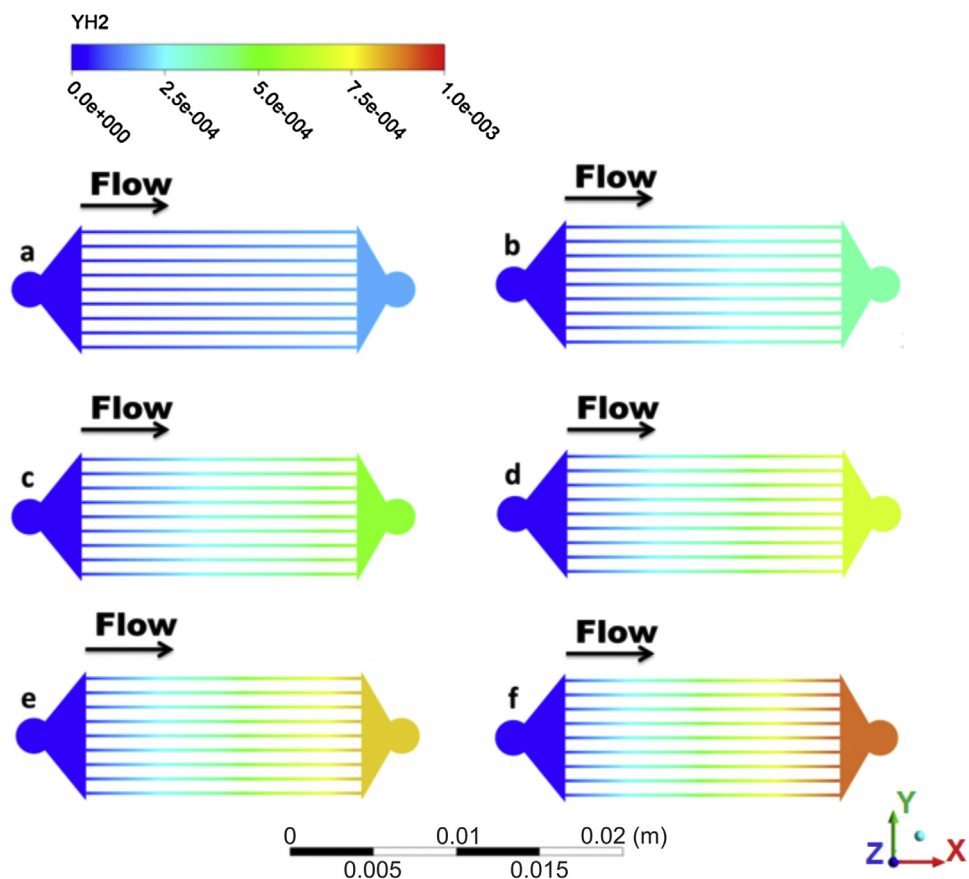


Fig. 7. H_2 yield maps in the single stack microreactor according to CFD simulations performed at $\text{GHSV} = 10,200 \text{ h}^{-1}$ with a gaseous $\text{H}_2\text{O:EtOH}$ feed stream mixture of 90:10 (molar basis) and the following irradiances: (a) 1.5 mW cm^{-2} , (b) 6 mW cm^{-2} , (c) 10 mW cm^{-2} , (d) 15 mW cm^{-2} , (e) 19 mW cm^{-2} and (f) 23 mW cm^{-2} .

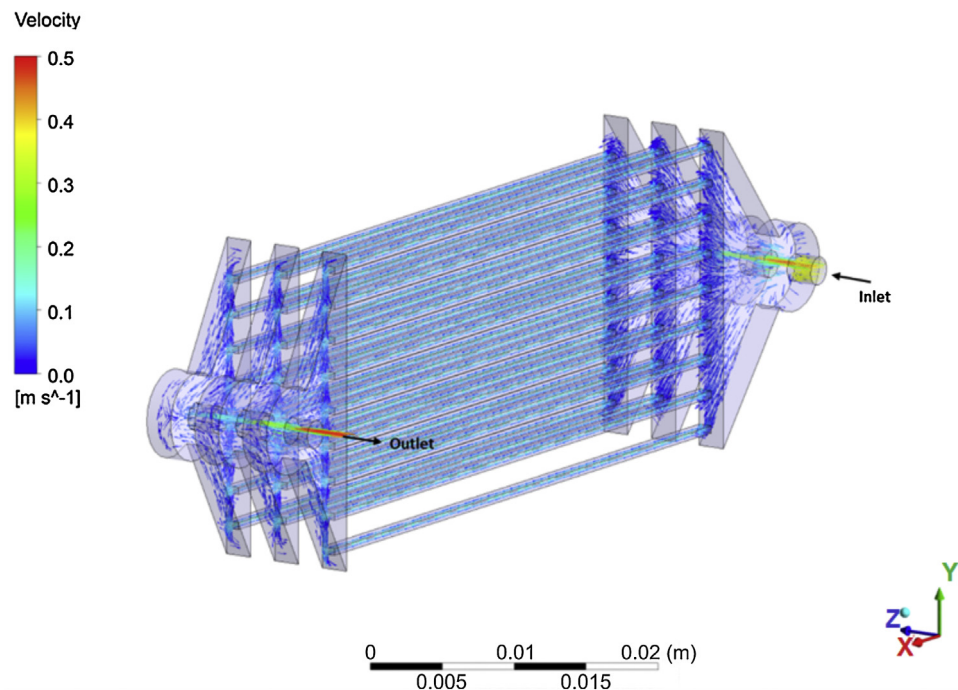


Fig. 8. Map of gas velocities obtained by means of CFD simulation at steady state of the triple stack microreactor operating at $\text{GHSV} = 3700 \text{ h}^{-1}$ with a feed stream containing a water:ethanol gaseous mixture of 90:10 (molar basis).

tion kinetics is still not saturated with respect to the irradiance level under the conditions selected in this study.

To gain further knowledge on how hydrogen is produced in the PDMS photocatalytic microreactors, the hydrogen yield (Y_{H_2}), defined according to the stoichiometry of the ethanol dehydrogenation reaction as the molar flow rate of hydrogen divided by the ethanol molar flow rate in the feed stream, has been calculated by means of CFD simulations and the results are shown in Fig. 7. It can be seen that the photoproduction of hydrogen progressively increases along the channels and that the hydrogen yield at the reactor exit is considerably higher as the irradiance increases. In this regard, the hydrogen production can be greatly enhanced in our case by using longer microchannels and, particularly by increasing the irradiance power well above the maximum value of 23 mW cm^{-2} considered in this study. However, if the irradiance power is increased, the quantum yield would likely decrease and, therefore, the kinetic parameter α could also decrease towards 0.5. Therefore, a compromise between irradiance power and a proper design of the microreactor for an effective absorption of light must be achieved.

4.2. Triple stack PDMS microreactor

Concerning the triple stack microreactor, a series of CFD simulations was first conducted in order to investigate the quality of the flow distribution at GHSV values ranging from 1000 to $15,300 \text{ h}^{-1}$. As a representative example, Fig. 8 shows the map of velocities at steady state for a GHSV value of 3700 h^{-1} . It can be seen that the flow distribution is very homogeneous and that almost identical velocity maps are obtained for the three stacks. A more detailed analysis revealed that the mean velocities at the microchannel inlets are slightly higher in the case of the stack that is closer to the inlet pipe, whereas the mean inlet velocities are almost the same for the channels of the other two stacks. Nevertheless, the velocities in the first stack ($0.097 \pm 0.002 \text{ m s}^{-1}$) are only about 5% greater than in the other two stacks. Moreover, this effect disappears as higher space velocities are used.

A second series of CFD simulations were performed and the results compared with the experimental data obtained with the three stack microreactor in order to validate the CFD model that incorporated the kinetic expression for the ethanol photocatalyzed dehydrogenation developed previously for the single stack. The water:ethanol gaseous mixtures (molar basis) used as feed stream were 99:1, 90:10, 80:20 and 50:50, and the residence time was fixed at 0.98 s (GHSV = 3700 h^{-1}).

The experimental and simulated hydrogen photoproduction of the triple stack microreactor are compared in Fig. 9. A good agreement between the experimental and CFD results can be observed in Fig. 9, which indicated that the mathematical model developed describes the performance of the photocatalytic microreactor reasonably well. However, the CFD model provides hydrogen photoproduction values that are slightly higher than those obtained experimentally, particularly at high irradiances and ethanol partial pressures. This small discrepancy is not strange because one can expect that the light intensity received by a stack decreases as the number of stacks placed above it increases. This effect has not been taken into account in the current CFD model but presumably it can be easily incorporated by means of a suitable correction factor of the light intensity received by each stack under working conditions.

Finally, the experimental specific hydrogen production rates (i.e. per gram of catalyst) of the triple ($\text{GHSV} = 10,200 \text{ h}^{-1}$) and single stack ($\text{GHSV} = 3700 \text{ h}^{-1}$) microreactors working under comparable conditions are shown in Fig. 10. It should be noted that the single stack has 9 microchannels whereas the triple stack contains 25 microchannels for achieving a better exposure to light. Therefore, the gas-hourly space velocities used in these experiments maintain

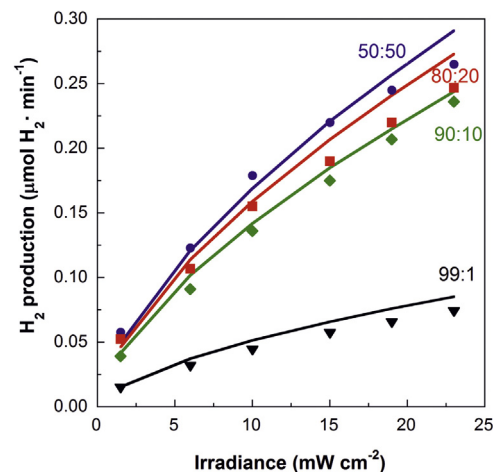


Fig. 9. Hydrogen photoproduction rates in the triple stack microreactor at different light irradiance values and $\text{H}_2\text{O:EtOH}$ molar ratios for $\text{GHSV} = 3700 \text{ h}^{-1}$. The symbols correspond to the experimental results and the lines to the CFD simulations.

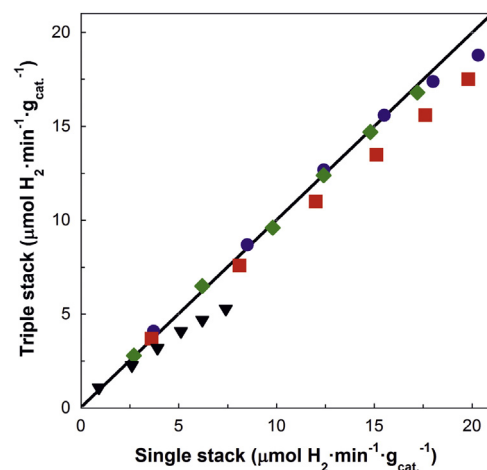


Fig. 10. Specific hydrogen production rates of the single stack ($\text{GHSV} = 3700 \text{ h}^{-1}$) and the triple stack ($\text{GHSV} = 10,200 \text{ h}^{-1}$) microreactors working at comparable conditions and $\text{H}_2\text{O:EtOH}$ molar ratios in the feed stream of 99:1 (triangles), 90:10 (diamonds), 80:20 (squares) and 50:50 (circles).

the same proportion as the one existing between the microchannel volumes of the microreactors. It can be seen that, in general, there is a good agreement among the results provided by both devices which points towards a relatively straightforward scale-up through numbering-up of this kind of microreactor. The small deviation observed under high light irradiation values for each water-ethanol reactant mixture can be attributed to the above-mentioned enhanced light absorption by PDMS in the triple stack configuration, which results in a slightly lower specific hydrogen production rates compared to the single stack.

5. Conclusions

The photocatalyzed conversion of bioethanol is a very interesting route for producing hydrogen of renewable origin. This process can be intensified by using suitable photocatalytic microreactors that allow an efficient use of the photons through a good contact between the photocatalyst and the reactants and a good exposure to the light. The recently reported effectiveness of these microdevices for hydrogen production through the photocatalytic dehydrogenation of bioethanol [13] is promising to develop future power applications. This work is a contribution to this approach in

which silicone microchannel reactors have been manufactured by 3D printing using Au/TiO₂ as the photocatalyst and high-efficacy LEDs as the light source. The results obtained with a single stack microreactor have demonstrated that the chemical kinetics are sufficiently described by a single rate equation of the Langmuir-Hinshelwood type in which the apparent kinetic constant depends on the light intensity as I^{0.65}. The kinetics also show a positive effect of the ethanol partial pressure although the reaction rate presents a saturation value with respect to this variable when a pressure of about 0.30 kPa is achieved (corresponding to 10 mol% of ethanol in the feed stream). Once the concept was satisfactorily validated, the microreactor was scaled up to a three stack device that contains a microchannel volume that is 2.7 times higher than that of the single stack microreactor. The specific (i.e. per gram of catalyst) hydrogen production rates of both microreactors were very similar, suggesting that the scale-up of this technology through numbering-up is relatively straightforward.

Computational fluid dynamics (CFD) models have been developed for both the single and triple stacks microreactors that incorporated the rate equation previously determined. CFD simulations revealed that the microreactor design allowed for a very homogeneous distribution of the gas stream among the channels. Moreover, the CFD models predicted the hydrogen production rates of the microreactors very well and they represent a very useful tool for scale-up purposes. Minor discrepancies between the simulated and predicted values can be attributed to the small fraction of the light that is absorbed by the PDMS used to fabricate the microreactors.

Acknowledgments

This work has been funded through MINECO grants and FEDER funding ENE2015-63969-R and ENE2015-66975-C3-1-R. JL is Serra Húnter Fellow and is grateful to ICREA Academia program. AC is grateful to MINECO for PhD grant BES-2013-065709. LS is grateful to Generalitat de Catalunya for a Beatriu de Pinós grant (2013 BP-B 00007).

References

- [1] M. Murdoch, G.I.N. Waterhouse, M.A. Nadeem, J.B. Metson, M.A. Keane, R.F. Howe, J. Llorca, H. Idriss, *Nat. Chem.* 3 (2011) 489–492.
- [2] J. Llorca, V. Cortés Corberán, N.J. Divins, R. Olivera Fraile, E. Taboada, in: L.M. Gandía, G. Arzamendi, P.M. Diéguez (Eds.), *Renew. Hydrot. Technol.*, Elsevier B.V., Oxford, UK, 2013, pp. 135–170.
- [3] A. Fujishima, K. Honda, *Nature* 238 (1972) 37–38.
- [4] T. Van Gerven, G. Mul, J. Moulijn, A. Stankiewicz, *Chem. Eng. Process. Process Intensif.* 46 (2007) 781–789.
- [5] K.F. Jensen, *Chem. Eng. Sci.* 56 (2001) 293–303.
- [6] N. Wang, X. Zhang, B. Chen, W. Song, N.Y. Chan, H.L.W. Chan, *Lab Chip* 12 (2012) 3983–3990.
- [7] S.S. Ahsan, A. Gumus, D. Erickson, *Lab Chip* 13 (2013) 409–414.
- [8] I. Salvadó-Estivill, D.M. Hargreaves, G.L. Puma, *Environ. Sci. Technol.* 41 (2007) 2028–2035.
- [9] I. Salvadó-Estivill, A. Brucato, G.L. Puma, *Ind. Eng. Chem. Res.* 46 (2007) 7489–7496.
- [10] E. Taboada, I. Angurell, J. Llorca, *J. Photochem. Photobiol. A Chem.* 281 (2014) 35–39.
- [11] E. Taboada, I. Angurell, J. Llorca, *J. Catal.* 309 (2014) 460–467.
- [12] E. Bonmatí, A. Casanovas, I. Angurell, J. Llorca, *Top. Catal.* 58 (2014) 77–84.
- [13] A. Castedo, E. Mendoza, I. Angurell, J. Llorca, *Catal. Today* 273 (2016) 106–111.
- [14] A. Visan, D. Rafieian, W. Ogieglo, R.G.H. Lammertink, *Appl. Catal. B Environ.* 150–151 (2014) 93–100.
- [15] I. Uriz, G. Arzamendi, P.M. Diéguez, L.M. Gandía, in: L.M. Gandía, G. Arzamendi, P.M. Diéguez (Eds.), *Renew. Hydrot. Technol.*, Elsevier B.V., Oxford, UK, 2013, pp. 401–436.
- [16] V. Jovic, W.T. Chen, D. Sun-Waterhouse, M.G. Blackford, H. Idriss, G.I.N. Waterhouse, *J. Catal.* 305 (2013) 307–317.
- [17] G.R. Bamwenda, S. Tsubota, T. Nakamura, M. Haruta, *J. Photochem. Photobiol. A Chem.* 89 (1995) 177–189.
- [18] J. Llorca, M. Domínguez, C. Ledesma, R.J. Chimentão, F. Medina, J. Sueiras, I. Angurell, M. Seco, O. Rossell, *J. Catal.* 258 (2008) 187–198.
- [19] I. Uriz, G. Arzamendi, P.M. Diéguez, F.J. Echave, O. Sanz, M. Montes, L.M. Gandía, *Chem. Eng. J.* 238 (2014) 37–44.
- [20] J.-M. Herrmann, E. Puzenat, in: M. Poux, P. Cognet, C. Gourdon (Eds.), *Green Process Eng. From Concepts to Ind. Appl.*, Dunod, Paris, 2010, pp. 364–395.
- [21] A.L. Pruden, D.F. Ollis, *J. Catal.* 82 (1983) 404–417.
- [22] A.K. Ray, A.A.C.M. Beenackers, *AIChE J.* 43 (1997) 2571–2578.
- [23] G. Arzamendi, I. Uriz, A. Navajas, P.M. Diéguez, L.M. Gandía, M. Montes, M.A. Centeno, J.M. Odriozola, *AIChE J.* 58 (2012) 2785–2797.
- [24] S. Walter, S. Malmberg, B. Schmidt, M.A. Liauw, *Catal. Today* 110 (2005) 15–25.